



Westinghouse Energy Systems



9102060188 910128
PDR ADOCK 05000327
P PDR

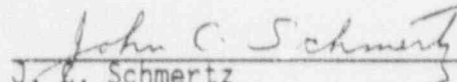
WCAP-12776

TECHNICAL JUSTIFICATION FOR ELIMINATING
PRESSURIZER SURGE LINE RUPTURE AS THE
STRUCTURAL DESIGN BASIS FOR
SEQUOYAH UNITS 1 AND 2

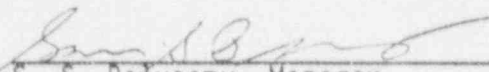
December 1990

	D. C. Bhowmick	
S. A. Swamy		Y. S. Lee
D. E. Prager		J. F. Petsche

Verified:


J. C. Schmertz
Structural Mechanics Technology

Approved:


S. S. Palusamy, Manager
Diagnostics and Monitoring Technology

Work Performed Under Shop Order: SZXP-9508

WESTINGHOUSE ELECTRIC CORPORATION
Nuclear and Advanced Technology Division
P.O. Box 2728
Pittsburgh, Pennsylvania 15230-2728

© 1990 Westinghouse Electric Corp.

TABLE OF CONTENTS

<u>Section</u>	<u>Title</u>	<u>Page</u>
1.0	INTRODUCTION	1-1
	1.1 Background	1-1
	1.2 Scope and Objective	1-1
	1.3 References	1-3
2.0	OPERATION AND STABILITY OF THE PRESSURIZER SURGE LINE AND THE REACTOR COOLANT SYSTEM	2-1
	2.1 Stress Corrosion Cracking	2-1
	2.2 Water Hammer	2-3
	2.3 Low Cycle and High Cycle Fatigue	2-4
	2.4 Summary Evaluation of Surge Line for Potential Degradation During Service	2-4
	2.5 References	2-5
3.0	MATERIAL CHARACTERIZATION	3-1
	3.1 Pipe and Weld Materials	3-1
	3.2 Material Properties	3-1
	3.3 References	3-2
4.0	LOADS FOR FRACTURE MECHANICS ANALYSIS	4-1
	4.1 Loads for Crack Stability Analysis	4-2
	4.2 Loads for Leak Rate Evaluation	4-2
	4.3 Loading Condition	4-2
	4.4 Summary of Loads Geometry and Materials	4-4
	4.5 Governing Locations	4-5

ABLE OF CONTENTS (cont.)

<u>Section</u>	<u>Title</u>	<u>Page</u>
5.0	FRACTURE MECHANICS EVALUATION	5-1
	5.1 Global Failure Mechanism	5-1
	5.2 Leak Rate Predictions	5-2
	5.3 Stability Evaluation	5-4
	5.4 References	5-5
6.0	ASSESSMENT OF FATIGUE CRACK GROWTH	6-1
	6.1 Introduction	6-1
	6.2 Initial Flaw Size	6-2
	6.3 Results of FCG Analysis	6-2
	6.4 References	6-3
7.0	ASSESSMENT OF MARGINS	7-1
8.0	CONCLUSIONS	8-1
APPENDIX A	Limit Moment	A-1

LIST OF TABLES

<u>Table</u>	<u>Title</u>	<u>Page</u>
3-1	Room Temperature Mechanical Properties of the Pressurizer Surge Line Materials and Welds of the Sequoyah Unit 1	3-3
3-2	Room Temperature Mechanical Properties of the Pressurizer Surge Line Materials and Welds of the Sequoyah Unit 2	3-4
3-3	Room Temperature ASME Code Minimum Properties	3-5
3-4	Representative Tensile Properties for Sequoyah Unit 1	3-6
3-5	Representative Tensile Properties for Sequoyah Unit 2	3-7
3-6	Modulus of Elasticity (E)	3-8
4-1	Types of Loadings	4-6
4-2	Normal and Faulted Loading Cases for Leak-Before Break Evaluations	4-7
4-3	Associated Load Cases for Analyses	4-8
4-4	Summary of LBB Loads and Stresses by Case for Sequoyah Unit 1	4-9
4-5	Summary of LBB Loads and Stresses by Case for Sequoyah Unit 2	4-10

LIST OF TABLES (cont.)

<u>Table</u>	<u>Title</u>	<u>Page</u>
5-1	Leak Rate Crack Length for Sequoyah Unit 1	5-6
5-2	Leak Rate Crack Length for Sequoyah Unit 2	5-7
5-3	Summary of Critical Flaw Size for Sequoyah Unit 1	5-8
5-4	Summary of Critical Flaw Size for Sequoyah Unit 2	5-9
6-1	Fatigue Crack Growth Results for 10% of Wall Initial Flaw Size	6-4
7-1	Leakage Flaw Sizes, Critical Flaw Sizes and Margins for Sequoyah Unit 1	7-2
7-2	Leakage Flaw Sizes, Critical Flaw Sizes and Margins for Sequoyah Unit 2	7-3
7-3	LBB Conservatism	7-4

LIST OF FIGURES

<u>Figure</u>	<u>Title</u>	<u>Page</u>
3-1	Sequoyah Unit 1 Surge Line Layout	3-9
3-2	Sequoyah Unit 2 Surge Line Layout	3-10
4-1	Sequoyah Unit 1 Surge Line Showing the Governing Locations	4-11
4-2	Sequoyah Unit 2 Surge Line Showing the Governing Locations	4-12
5-1	Fully Plastic Stress Distribution	5-10
5-2	Analytical Predictions of Critical Flow Rates of Steam-Water Mixtures	5-11
5-3	[$j^{a,c,e}$ Pressure Ratio as a Function of L/D	5-12
5-4	Idealized Pressure Drop Profile through a Postulated Crack	5-13
5-5	Loads Acting on the Model at the Governing Location	5-14
5-6	Critical Flaw Size Prediction for Sequoyah Unit 1 Node 1020 Case D	5-15
5-7	Critical Flaw Size Prediction for Sequoyah Unit 1 Node 1020 Case E	5-16
5-8	Critical Flaw Size Prediction for Sequoyah Unit 1 Node 1020 Case F	5-17

LIST OF FIGURES (cont.)

<u>Figure</u>	<u>Title</u>	<u>Page</u>
5-9	Critical Flaw Size Prediction for Sequoyah Unit 1 Node 1020 Case G	5-18
5-10	Critical Flaw Size Prediction for Sequoyah Unit 1 Node 1080 Case D	5-19
5-11	Critical Flaw Size Prediction for Sequoyah Unit 1 Node 1080 Case E	5-20
5-12	Critical Flaw Size Prediction for Sequoyah Unit 1 Node 1080 Case F	5-21
5-13	Critical Flaw Size Prediction for Sequoyah Unit 1 Node 1080 Case G	5-22
5-14	Critical Flaw Size Prediction for Sequoyah Unit 2 Node 1020 Case D	5-23
5-15	Critical Flaw Size Prediction for Sequoyah Unit 2 Node 1020 Case E	5-24
5-16	Critical Flaw Size Prediction for Sequoyah Unit 2 Node 1020 Case F	5-25
5-17	Critical Flaw Size Prediction for Sequoyah Unit 2 Node 1020 Case G	5-26
5-18	Critical Flaw Size Prediction for Sequoyah Unit 2 Node 1080 Case D	5-27
5-19	Critical Flaw Size Prediction for Sequoyah Unit 2 Node 1080 Case E	5-28

LIST OF FIGURES (cont.)

<u>Figure</u>	<u>Title</u>	<u>Page</u>
5-20	Critical Flaw Size Prediction for Sequoyah Unit 2 Node 1080 Case F	5-29
5-21	Critical Flaw Size Prediction for Sequoyah Unit 2 Node 1080 Case G	5-30
6-1	Determination of the Effects of Thermal Stratification on Fatigue Crack Growth	6-5
6-2	Fatigue Crack Growth Methodology	6-6
6-3	Fatigue Crack Growth Rate Curve for Austenitic Stainless Steel	6-7
6-4	Fatigue Crack Growth Rate Equation for Austenitic Stainless Steel	6-8
6-5	Fatigue Crack Growth Critical Locations	6-9
A-1	Pipe with a Through-Wall Crack in Bending	A-3

SECTION 1.0 INTRODUCTION

1.1 Background

The current structural design basis for the pressurizer surge line requires postulating non-mechanistic circumferential and longitudinal pipe breaks. This results in additional plant hardware (e.g. pipe whip restraints and jet shields) which would mitigate the dynamic consequences of the pipe breaks. It is, therefore, highly desirable to be realistic in the postulation of pipe breaks for the surge line. Presented in this report are the descriptions of a mechanistic pipe break evaluation method and the analytical results that can be used for establishing that a circumferential type break will not occur within the pressurizer surge line. The evaluations considering circumferentially oriented flaws cover longitudinal cases. The pressurizer surge line is known to be subjected to thermal stratification and the effects of thermal stratification for Sequoyah surge lines have been evaluated and documented in WCAP-12777. The results of the stratification evaluation as described in WCAP-12777 have been used in the leak-before-break evaluation presented in this report.

1.2 Scope and Objective

The general purpose of this investigation is to demonstrate leak-before-break for the pressurizer surge line. The scope of this work covers the entire pressurizer surge line from the primary loop nozzle junction to the pressurizer nozzle junction. A schematic drawing of the piping system is shown in Section 3.0. The recommendations and criteria proposed in NUREG 1061 Volume 3 (1-1) are used in this evaluation. The criteria and the resulting steps of the evaluation procedure can be briefly summarized as follows:

- 1) Calculate the applied loads. Identify the location at which the highest stress occurs.
- 2) Identify the materials and the associated material properties.

- 3) Postulate a surface flaw at the governing location. Determine fatigue crack growth. Show that a through-wall crack will not result.
- 4) Postulate a through-wall flaw at the governing location. The size of the flaw should be large enough so that the leakage is assured of detection with margin using the installed leak detection equipment when the pipe is subjected to normal operating loads. A margin of 10 is demonstrated between the calculated leak rate and the leak detection capability.
- 5) Using maximum faulted loads, demonstrate that there is a margin of at least 2 between the leakage size flaw and the critical size flaw.
- 6) Review the operating history to ascertain that operating experience has indicated no particular susceptibility to failure from the effects of corrosion, water hammer or low and high cycle fatigue.
- 7) For the base and weld metals actually in the plant provide the material properties including toughness and tensile test data. Justify that the properties used in the evaluation are representative of the plant specific material. Evaluate long term effects such as thermal aging where applicable.
- 8) Demonstrate margin on applied load.

The flaw stability analyses is performed using the methodology described in SRP 3.6.3 (1-2).

The leak rate is calculated for the normal operating condition. The leak rate prediction model used in this evaluation is an [

]a,c,e The crack opening area required for calculating the leak rates is obtained by subjecting the postulated through-wall flaw to normal operating loads (1-3). Surface roughness is accounted for in determining the leak rate through the postulated flaw.

1.2 References

- 1-1 Report of the U.S. Nuclear Regulatory Commission Piping Review Committee - Evaluation of Potential for Pipe Breaks, NUREG 1061, Volume 3, November 1984.
- 1-2 Standard Review Plan; public comments solicited; 3.6.3 Leak-Before-Break Evaluation Procedures; Federal Register/Vol. 52, No. 167/Friday, August 28, 1987/Notices, pp. 32626-32633.
- 1-3 NUREG/CR-3464, 1983, "The Application of Fracture Proof Design Methods Using Tearing Instability Theory to Nuclear Piping Postulated Circumferential Through Wall Cracks."

SECTION 2.0

OPERATION AND STABILITY OF THE PRESSURIZER SURGE LINE AND THE REACTOR COOLANT SYSTEM

2.1 Stress Corrosion Cracking

The Westinghouse reactor coolant system primary loop and connecting Class 1 lines have an operating history that demonstrates the inherent operating stability characteristics of the design. This includes a low susceptibility to cracking failure from the effects of corrosion (e.g., intergranular stress corrosion cracking). This operating history totals over 400 reactor-years, including five plants each having over 15 years of operation and 15 other plants each with over 10 years of operation.

In 1978, the United States Nuclear Regulatory Commission (USNRC) formed the second Pipe Crack Study Group. (The first Pipe Crack Study Group established in 1975 addressed cracking in boiling water reactors only.) One of the objectives of the second Pipe Crack Study Group (PCSG) was to include a review of the potential for stress corrosion cracking in Pressurized Water Reactors (PWR's). The results of the study performed by the PCSG were presented in NUREG-0531 (Reference 2-1) entitled "Investigation and Evaluation of Stress Corrosion Cracking in Piping of Light Water Reactor Plants." In that report the PCSG stated:

"The PCSG has determined that the potential for stress-corrosion cracking in PWR primary system piping is extremely low because the ingredients that produce IGSCC are not all present. The use of hydrazine additives and a hydrogen overpressure limit the oxygen in the coolant to very low levels. Other impurities that might cause stress-corrosion cracking, such as halides or caustic, are also rigidly controlled. Only for brief periods during reactor shutdown when the coolant is exposed to the air and during the subsequent startup are conditions even marginally capable of producing stress-corrosion cracking in the primary systems of PWRs.

Operating experience in PWRs supports this determination. To date, no stress-corrosion cracking has been reported in the primary piping or safe ends of any PWR."

During 1979, several instances of cracking in PWR feedwater piping led to the establishment of the third PCSG. The investigations of the PCSG reported in NUREG-0691 (Reference 2-2) further confirmed that no occurrences of IGSCC have been reported for PWR primary coolant systems.

As stated above, for the Westinghouse plants there is no history of cracking failure in the reactor coolant system loop or connecting Class 1 piping. The discussion below further qualifies the PCSG's findings.

For stress corrosion cracking (SCC) to occur in piping, the following three conditions must exist simultaneously: high tensile stresses, susceptible material, and a corrosive environment. Since some residual stresses and some degree of material susceptibility exist in any stainless steel piping, the potential for stress corrosion is minimized by properly selecting a material immune to SCC as well as preventing the occurrence of a corrosive environment. The material specifications consider compatibility with the system's operating environment (both internal and external) as well as other material in the system, applicable ASME Code rules, fracture toughness, welding, fabrication, and processing.

The elements of a water environment known to increase the susceptibility of austenitic stainless steel to stress corrosion are: oxygen, fluorides, chlorides, hydroxides, hydrogen peroxide, and reduced forms of sulfur (e.g., sulfides, sulfites, and thionates). Strict pipe cleaning standards prior to operation and careful control of water chemistry during plant operation are used to prevent the occurrence of a corrosive environment. Prior to being put into service, the piping is cleaned internally and externally. During flushes and preoperational testing, water chemistry is controlled in accordance with written specifications. Requirements on chlorides, fluorides, conductivity, and pH are included in the acceptance criteria for the piping.

During plant operation, the reactor coolant water chemistry is monitored and maintained within very specific limits. Contaminant concentrations are kept below the thresholds known to be conducive to stress corrosion cracking with the major water chemistry control standards being included in the plant operating procedures as a condition for plant operation. For example, during normal power operation, oxygen concentration in the RCS and connecting Class 1 lines is expected to be in the ppb range by controlling charging flow chemistry and maintaining hydrogen in the reactor coolant at specified concentrations. Halogen concentrations are also stringently controlled by maintaining concentrations of chlorides and fluorides within the specified limits. This is assured by controlling charging flow chemistry. Thus during plant operation, the likelihood of stress corrosion cracking is minimized.

2.2 Water Hammer

Overall, there is a low potential for water hammer in the RCS and connecting surge lines since they are designed and operated to preclude the voiding condition in normally filled lines. The RCS and connecting surge line including piping and components, are designed for normal, upset, emergency, and faulted condition transients. The design requirements are conservative relative to both the number of transients and their severity. Relief valve actuation and the associated hydraulic transients following valve opening are considered in the system design. Other valve and pump actuations are relatively slow transients with no significant effect on the system dynamic loads. To ensure dynamic system stability, reactor coolant parameters are stringently controlled. Temperature during normal operation is maintained within a narrow range by control rod position; pressure is controlled by pressurizer heaters and pressurizer spray also within a narrow range for steady-state conditions. The flow characteristics of the system remain constant during a fuel cycle because the only governing parameters, namely system resistance and the reactor coolant pump characteristics are controlled in the design process. Additionally, Westinghouse has instrumented typical reactor coolant systems to verify the flow and vibration characteristics of the system and connecting surge lines. Preoperational testing and operating experience have verified the Westinghouse approach. The operating transients

of the RCS primary piping and connected surge lines are such that no significant water hammer can occur.

2.3 Low Cycle and High Cycle Fatigue

Low cycle fatigue considerations are accounted for in the design of the piping system through the fatigue usage factor evaluation to show compliance with the rules of Section III of the ASME Code. A further evaluation of the low cycle fatigue loading is discussed in Section 6.0 as part of this study in the form of a fatigue crack growth analysis.

Pump vibrations during operation would result in high cycle fatigue loads in the piping system. During operation, an alarm signals the exceedance of the RC pump shaft vibration limits. Field measurements have been made on the reactor coolant loop piping of a number of plants during hot functional testing. Stresses in the elbow below the RC pump have been found to be very small, between 2 and 3 ksi at the highest. Recent field measurements on typical PWR plants indicate vibration amplitudes less than 1 ksi. When translated to the connecting surge line, these stresses would be even lower, well below the fatigue endurance limit for the surge line material and would result in an applied stress intensity factor below the threshold for fatigue crack growth.

2.4 Summary Evaluation of Surge Line for Potential Degradation During Service

There has never been any service cracking or wall thinning identified in the pressurizer surge lines of Westinghouse PWR design. Sources of such degradation are mitigated by the design, construction, inspection, and operation of the pressurizer surge piping.

There is no mechanism for water hammer in the pressurizer/surge system. The pressurizer safety and relief piping system which is connected to the top of the pressurizer could have loading from water hammer events. However, these loads are effectively mitigated by the pressurizer and have a negligible effect on the surge line.

Wall thinning by erosion and erosion-corrosion effects will not occur in the surge line due to the low velocity, typically less than 1.0 ft/sec and the material, austenitic stainless steel, which is highly resistant to these degradation mechanisms. Per NUREG-0691, a study of pipe cracking in PWR piping, only two incidents of wall thinning in stainless steel pipe were reported and these were not in the surge line. Although it is not clear from the report, the cause of the wall thinning was related to the high water velocity and is therefore clearly not a mechanism which would affect the surge line.

It is well known that the pressurizer surge lines are subjected to thermal stratification and the effects of stratification are particularly significant during certain modes of heatup and cooldown operation. The effects of stratification have been evaluated for the Sequoyah plant surge lines and the loads, accounting for the stratification effects, have been derived in WCAP-12777. These loads are used in the leak-before-break evaluation described in this report.

The Sequoyah Units 1 & 2 surge line piping and associated fittings are forged product forms (see Section 3) which are not susceptible to toughness degradation due to thermal aging.

Finally, the maximum operating temperature of the pressurizer surge piping, which is about 650°F, is well below the temperature which would cause any creep damage in stainless steel piping.

2.5 References

- 2-1 Investigation and Evaluation of Stress-Corrosion Cracking in Piping of Light Water Reactor Plants, NUREG-0531, U.S. Nuclear Regulatory Commission, February 1979.
- 2-2 Investigation and Evaluation of Cracking Incidents in Piping in Pressurized Water Reactors, NUREG-0691, U.S. Nuclear Regulatory Commission, September 1980.

SECTION 3.0 MATERIAL CHARACTERIZATION

3.1 Pipe and Weld Materials

The pipe material of the pressurizer surge line for the Sequoyah Units 1 & 2 is A376/TP316. These are a wrought product form of the type used for the primary loop piping of several PWR plants. The surge line is connected to the primary loop nozzle at one end and the other end of the surge line is connected to the pressurizer nozzle. The surge line system does not include any cast pipe or cast fitting. The welding processes used are shielded metal arc (SMAW) and submerged arc (SAW). Weld locations are identified in Figures 3-1 and 3-2.

In the following section the tensile properties of the materials are presented for use in the leak-before-break analyses.

3.2 Material Properties

The room temperature mechanical properties of the Sequoyah Units 1 & 2 surge line materials were obtained from the Certified Materials Test Reports and are given in Table 3-1 and 3-2. The room temperature ASME Code minimum properties are given in Table 3-3. It is seen that the measured properties well exceed those of the Code. The representative minimum and average tensile properties were established from the Certified Material Test Report. The material properties at temperatures (135°F, 205°F, 300°F, 330°F and 653°F) are required for the leak rate and stability analyses discussed later. The minimum and average tensile properties were calculated by using the ratio of the ASME Section III properties at the temperatures of interest stated above. Tables 3-4 and 3-5 show the tensile properties at various temperatures for the Sequoyah Units 1 & 2. The modulus of elasticity values were established at various temperatures from the ASME Section III (Table 3-6). In the leak-before-break evaluation, the representative minimum properties at

temperature are used for the flaw stability evaluations and the representative average properties are used for the leak rate predictions. The minimum ultimate stresses are used for stability analyses. These properties are summarized in Tables 3-4 and 3-5.

3.3 References

- 3-1 ASME Boiler and Pressure Vessel Code Section III, Division 1, Appendices July 1, 1989.

TABLE 3-1

Room Temperature Mechanical Properties of the Pressurizer Surge Line
Materials and Welds of the Sequoyah Unit 1

ID	HEAT NO./SERIAL NO.	MATERIAL	ULTIMATE	YIELD	ELONG.	R/A
			STRENGTH	STRENGTH		
			psi	psi	(%)	(%)
1	J2469/6559	A376/TP316	86,100	43,700	51.4	67.5
			83,400	42,400	52.5	72.3
2	J2471/6551	A376/TP316	83,400	41,800	53.1	69.3
			84,300	39,900	50.8	65.7
3	J2617/7044	A376/TP316	85,900	42,500	50.5	65.9
			88,400	43,900	50.0	63.5
4	J2469/6538	A376/TP316	87,400	44,900	51.7	73.0
			87,100	48,000	47.2	67.3
5	J2469/6538	A376/TP316	87,400	44,900	51.7	73.0
			87,100	48,000	47.2	67.3

SW - Shop Weld

: All shop welds were fabricated by SAW

FW - Field Weld

: All field welds were fabricated by GTAW and SMAW combination

TABLE 3-2

Room Temperature Mechanical Properties of the Pressurizer Surge Line
Materials and Welds of the Sequoyah Unit 2

ID	HEAT NO./SERIAL NO.	MATERIAL	ULTIMATE	YIELD	ELONG.	R/A
			STRENGTH	STRENGTH		
			psi	psi	(%)	(%)
1	J2471/6553	A376/TP316	83,600	41,800	50.0	68.2
			83,600	41,800	51.4	68.2
2	J2469/6562	A376/TP316	83,600	41,800	52.2	71.4
			83,500	40,800	52.5	66.8
3	J2469/6562	A376/TP316	83,600	41,800	52.2	71.4
			83,500	40,800	52.5	66.8
4	J2470/6541	A376/TP316	83,000	41,600	50.9	69.9
			83,900	40,700	53.5	68.9

SW - Shop Weld

: All shop welds were fabricated by SAW

FW - Field Weld

: All field welds were fabricated by GTAW and SMAW combination

TABLE 3-3

Room Temperature ASME Code Minimum Properties

<u>Material</u>	<u>Yield Stress</u> (psi)	<u>Ultimate Stress</u> (psi)
A376/TP316	30,000	75,000

TABLE 3-4

Representative Tensile Properties for Sequoyah Unit 1

<u>Material</u>	<u>Temperature (°F)</u>	<u>Minimum Yield (psi)</u>	<u>Average Yield (psi)</u>	<u>Minimum Ultimate (psi)</u>
A376/TP316	100	39,900	44,000	83,400
	135	37,940	41,840	83,400
	205	34,150	37,660	83,300
	300	30,990	34,170	81,620
	330	30,230	33,330	81,080
	653	24,570	27,100	79,840

TABLE 3-5

Representative Tensile Properties for Sequoyah Unit 2

<u>Material</u>	<u>Temperature (°F)</u>	<u>Minimum Yield (psi)</u>	<u>Average Yield (psi)</u>	<u>Minimum Ultimate (psi)</u>
A376/TP316	100	40,700	41,390	83,000
	135	38,710	39,360	83,000
	205	34,840	35,430	82,910
	300	31,600	32,140	81,220
	330	30,830	31,360	80,690
	653	25,070	25,490	79,460

TABLE 3-6

Modulus of Elasticity (E)

<u>Temperature</u> (°F)	<u>E (ksi)</u>
100	28,138
135	27,950
205	27,600
300	27,050
330	26,885
653	25,035





4857a/111590 10

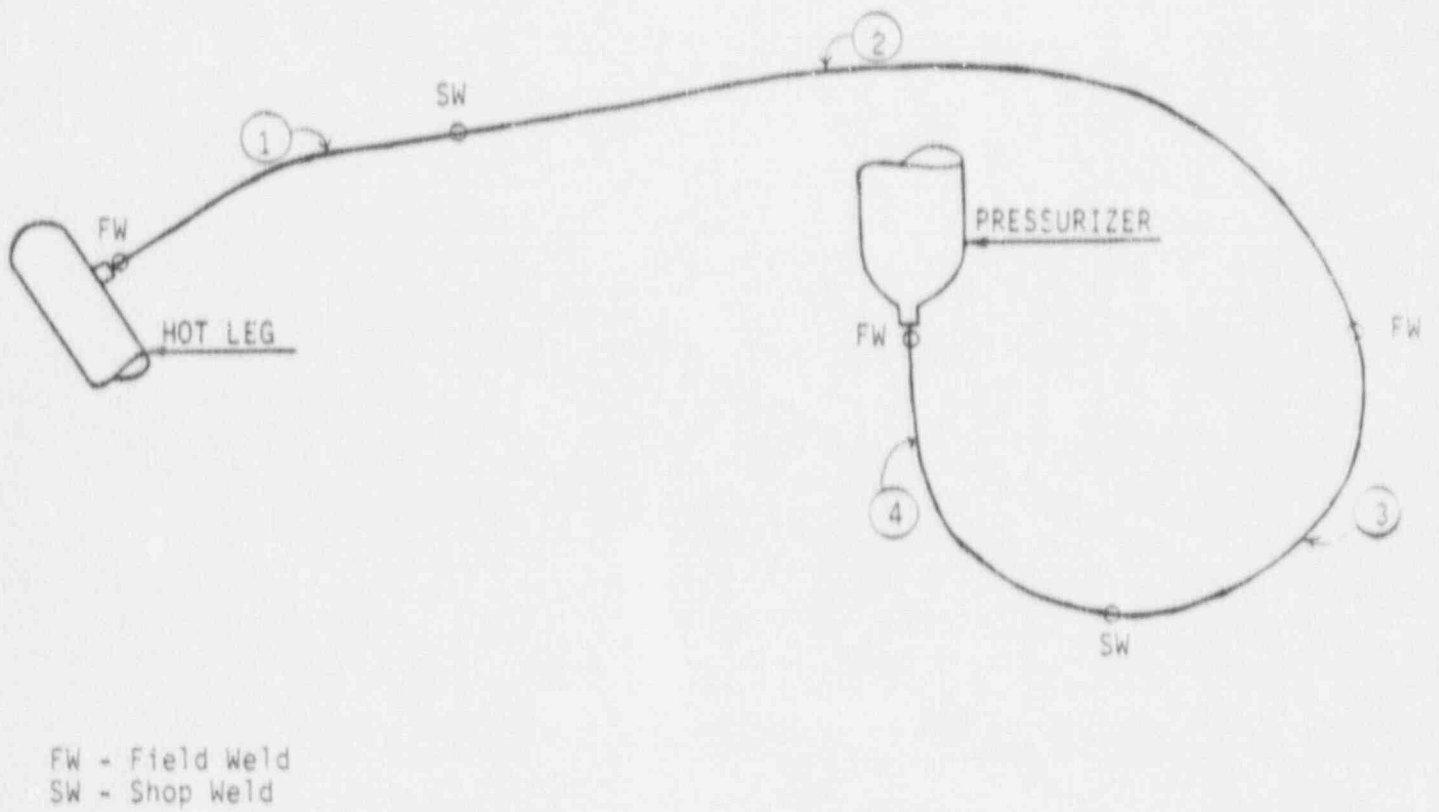


Figure 3-2 Sequoyah Unit 2 Surge Line Layout

SECTION 4.0

LOADS FOR FRACTURE MECHANICS ANALYSIS

Figures 3-1 and 3-2 show schematic layouts of the surge lines for Sequoyah Units 1 & 2 and identify the weld locations.

The stresses due to axial loads and bending moments were calculated by the following equation:

$$\sigma = \frac{F}{A} + \frac{M}{Z} \quad (4-1)$$

where,

σ	=	stress
F	=	axial load
M	=	bending moment
A	=	metal cross-sectional area
Z	=	section modulus

The bending moments for the desired loading combinations were calculated by the following equation:

$$M_B = (M_Y^2 + M_Z^2)^{0.5} \quad (4-2)$$

where,

M_B	=	bending moment for required loading
M_Y	=	Y component of bending moment
M_Z	=	Z component of bending moment

The axial load and bending moments for crack stability analysis and leak rate predictions are computed by the methods to be explained in Sections 4.1 and 4.2 which follow.

4.1 Loads for Crack Stability Analysis

The faulted loads for the crack stability analysis were calculated by the following equations:

$$F = |F_{DW}| + |F_{TH}| + |F_P| + |F_{SSE}| \quad (4-3)$$

$$M_Y = |(M_Y)_{DW}| + |(M_Y)_{TH}| + |M_Y \text{ SSE}| \quad (4-4)$$

$$M_Z = |(M_Z)_{DW}| + |(M_Z)_{TH}| + |M_Z \text{ SSE}| \quad (4-5)$$

DW = Deadweight

TH = Applicable thermal load (normal or stratified)

P = Load due to internal pressure

SSE = SSE loading including seismic anchor motion

4.2 Loads for Leak Rate Evaluation

The normal operating loads for leak rate predictions were calculated by the following general equations:

$$F = F_{DW} + F_{TH} + F_P \quad (4-6)$$

$$M_Y = (M_Y)_{DW} + (M_Y)_{TH} \quad (4-7)$$

$$M_Z = (M_Z)_{DW} + (M_Z)_{TH} \quad (4-8)$$

The parameters and subscripts are the same as those explained in Section 4.1.

4.3 Loading Conditions

Because thermal stratification can cause large stresses at heatup and cooldown temperatures in the range of 455°F, a review of stresses was used to identify the worst situations for LBB applications. The loading states so identified are given in Table 4-1.

Seven loading cases were identified for LBB evaluation as given in Table 4-2. Cases A, B, C are cases for leak rate calculations with the remaining cases being the corresponding faulted situations for stability evaluations.

The cases postulated for leak-before-break are summarized in Table 4-3. The cases of primary interest are the postulation of a detectable leak at normal power conditions [

]a,c,e

The combination [

]a,c,e

The more realistic cases [

]a,c,e

[

]a,c,e The logic for this ΔT []a,c,e

is based on the following:

Actual practice, based on experience of other plants with this type of situation, indicates that the plant operators complete the cooldown as quickly as possible once a leak in the primary system is detected. Technical Specifications may require cold shutdown within 36 hours but actual practice is that the plant depressurizes the system as soon as possible once a primary system leak is detected. Therefore, the hot leg is generally on the warmer side of the limits ($\sim 200^\circ\text{F}$) when the pressurizer bubble is quenched. Once the bubble is quenched, the pressurizer is cooled down fairly quickly reducing the ΔT in the system.

4.4 Summary of Loads and Geometry

The load combinations were evaluated at the various weld locations. Normal loads were determined using the algebraic sum method whereas faulted loads were combined using the absolute sum method.

4.5 Governing Locations

All the welds at Sequoyah Units 1 and 2 surge lines are fabricated using the SMAW and SAW procedure. The following governing locations were established for each type of the weld.

SMAW Weld

Node 1020 (hot leg nozzle junction) for Sequoyah Units 1 and 2

SAW Weld

Node 1080 for Sequoyah Units 1 and 2

The loads and stresses at these critical locations for all the loading combinations are shown in Tables 4-4 and 4-5.

Figure 4-1 and 4-2 show the governing locations.

TABLE 4-1

Types of Loadings

Pressure (P)

Dead Weight (DW)

Normal Operating Thermal Expansion (TH)

Safe Shutdown Earthquake and Seismic Anchor Motion (SSE)^a

a, c, e

^aSSE is used to refer to the absolute sum of these loadings.

TABLE 4-2

Normal and Faulted Loading Cases for Leak-Before-Break Evaluations

CASE A: This is the normal operating case at 653°F consisting of the algebraic sum of the loading components due to P, DW and TH.

CASE B:	[]	a.c.e
CASE C:			

CASE D: This is the faulted operating case at 653°F consisting of the absolute sum (every component load is taken as positive) of P, DW, TH and SSE.

CASE E:	[]	a.c.e
CASE F:			
CASE G:			

TABLE 4-3

Associated Load Cases for Analyses

A/D This is here-to-fore standard leak-before-break evaluation.

A/F	a, c, e
B/E	
B/F	
B/G ^a	
C/G ^a	

^a These are judged to be low probability events.

TABLE 4-4

Summary of LBB Loads and Stresses by Case for Sequoyah Unit 1

Node	Case	F_X (lbs)	S_X (psi)	M_B (in-lb)	S_B (psi)	S_T (psi)	
1020	A	251742	5025	1642805	11191	16216	a, c, e
1020							
1020							
1020	D	258370	5157	2122075	14456	19613	a, c, e
1020							
1020							
1080	A	248830	4967	628052	4278	9245	a, c, e
1080							
1080							
1080	D	253777	5065	1586229	11487	16552	a, c, e
1080							
1080							

TABLE 4-5

Summary of LBB Loads and Stresses by Case for Sequoyah Unit 2

Node	Case	F_X (lbs)	S_X (psi)	M_D (in-lb)	S_B (psi)	S_T (psi)	
1020	A	251742	5025	1642805	11191	16216	a.c.e
1020							
1020							
1020	D	258370	5157	2122075	14456	19613	a.c.e
1020							
1020							
1080	A	248830	4967	628052	4278	9245	a.c.e
1080							
1080							
1080	D	253777	5065	1686229	11487	16552	a.c.e
1080							
1080							

- o Pipe 14" Schedule 160
- o Minimum Wall Thickness is 1.251"

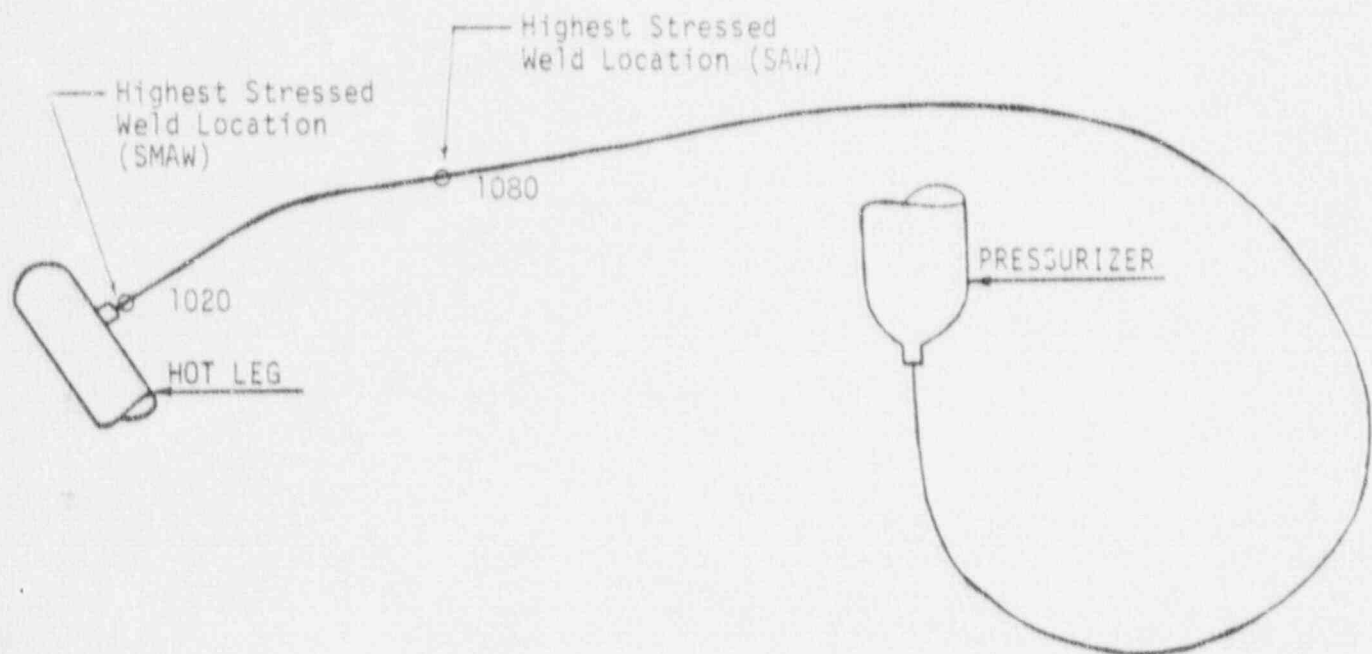


Figure 4-1 Sequoyah Unit 1 Surge Line
Showing Governing Locations

- o Pipe 14" Schedule 160
- o Minimum Wall Thickness is 1.251"

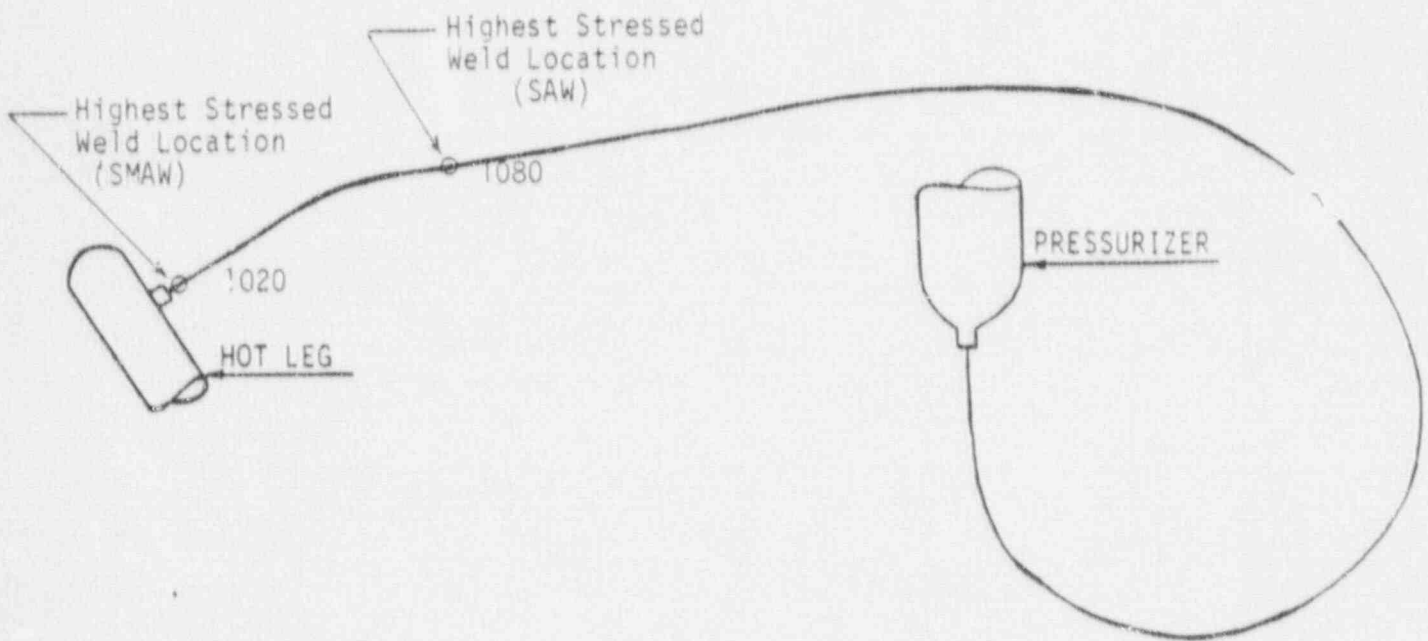


Figure 4-2 Sequoyah Unit 2 Surge Line
Showing Governing Locations

SECTION 5.0 FRACTURE MECHANICS EVALUATION

5.1 Global Failure Mechanism

Determination of the conditions which lead to failure in stainless steel should be done with plastic fracture methodology because of the large amount of deformation accompanying fracture. One method for predicting the failure of ductile material is the []^{a,c,e} method, based on traditional plastic limit load concepts, but accounting for []^{a,c,e} and taking into account the presence of a flaw. The flawed component is predicted to fail when the remaining net section reaches a stress level at which a plastic hinge is formed. The stress level at which this occurs is termed as the flow stress. [

]^{a,c,e} This methodology has been shown to be applicable to ductile piping through a large number of experiments and is used here to predict the critical flaw size in the pressurizer surge line. The failure criterion has been obtained by requiring equilibrium of the section containing the flaw (Figure 5-1) when loads are applied. The detailed development is provided in Appendix A for a through-wall circumferential flaw in a pipe section with internal pressure, axial force, and imposed bending moments. The limit moment for such a pipe is given by:

$$[\quad]^{a,c,e} \quad (5-1)$$

where:

[

]^{a,c,e}

$j_{a,c,e}$

(5-2)

The analytical model described above accurately accounts for the internal pressure as well as imposed axial force as they affect the limit moment. Good agreement was found between the analytical predictions and the experimental results (reference 5-1). Flaw stability evaluations, using this analytical model, are presented in section 5.3.

5.2 Leak Rate Predictions

Fracture mechanics analysis shows in general that postulated through-wall cracks in the surge line would remain stable and do not cause a gross failure of this component. However, if such a through-wall crack did exist, it would be desirable to detect the leakage such that the plant could be brought to a safe shutdown condition. The purpose of this section is to discuss the method which will be used to predict the flow through such a postulated crack and present the leak rate calculation results for through-wall circumferential cracks.

5.2.1 General Considerations

The flow of hot pressurized water through an opening to a lower back pressure (causing choking) is taken into account. For long channels where the ratio of the channel length, L , to hydraulic diameter, D_H , (L/D_H) is greater than $[j]_{a,c,e}$, both $[j]_{a,c,e}$ and $[j]_{a,c,e}$ must be considered.

In this situation the flow can be described as being single-phase through the channel until the local pressure equals the saturation pressure of the fluid.

At this point, the flow begins to flash and choking occurs. Pressure losses due to momentum changes will dominate for $[j^{a,c,e}]$. However, for large L/D_H values, the friction pressure drop will become important and must be considered along with the momentum losses due to flashing.

5.2.2 Calculational Method

In using the $[j^{a,c,e}]$

$$j^{a,c,e}$$

The flow rate through a crack was calculated in the following manner. Figure 5-2 from reference 5-2 was used to estimate the critical pressure, P_c , for the primary loop enthalpy condition and an assumed flow. Once P_c was found for a given mass flow, the $[j^{a,c,e}]$ was found from figure 5-3 taken from reference 5-2. For all cases considered, since $[j^{a,c,e}]$ Therefore, this method will yield the two-phase pressure drop due to momentum effects as illustrated in figure 5-4. Now using the assumed flow rate, G , the frictional pressure drop can be calculated using

$$\Delta P_f = [j^{a,c,e}]^2 \quad (5-3)$$

where the friction factor f is determined using the $[j^{a,c,e}]$. The crack relative roughness, ϵ , was obtained from fatigue crack data on stainless steel samples. The relative roughness value used in these calculations was $[j^{a,c,e}]_{RMS}$.

The frictional pressure drop using Equation 5-3 is then calculated for the assumed flow and added to the [Fauske model]^{a,c,e} to obtain the total pressure drop from the system under consideration to the atmosphere. Thus,

$$\text{Absolute Pressure} - 14.7 = [\quad]^{a,c,e} \quad (5-4)$$

for a given assumed flow G. If the right-hand side of equation 5-4 does not agree with the pressure difference between the piping under consideration and the atmosphere, then the procedure is repeated until equation 5-4 is satisfied to within an acceptable tolerance and this results in the flow value through the crack.

5.2.3 Leak Rate Calculations

Leak rate calculations were performed as a function of postulated through-wall crack length for the critical locations previously identified. The crack opening area was estimated using the method of reference 5-3 and the leak rates were calculated using the calculational methods described above. The leak rates were calculated using the normal operating loads at the governing nodes identified in section 4.0. The crack lengths yielding a leak rate of 10 gpm (10 times the leak detection capability of 1.0 gpm) for critical location at the Sequoyah Unit 1 & 2 pressurizer surge lines are shown in Tables 5-1 and 5-2.

5.3 Stability Evaluation

A typical segment of the nozzle under maximum loads of axial force F and bending moment M is schematically illustrated as shown in figure 5-5. In order to calculate the critical flaw size, plots of the limit moment versus crack length are generated as shown in figures 5-6 to 5-21. The critical flaw size corresponds to the intersection of this curve and the maximum load line. The critical flaw size is calculated using the lower bound base metal tensile properties established in section 3.0.

The weld at the locations of interest (i.e. the governing location) are SMAW welds. Therefore, "Z" factor corrections for SMAW and SAW welds were applied (references 5-4 and 5-5) as follows:

$$Z = 1.15 [1 + 0.013 (O.D. - 4)] \text{ (for SMAW)} \quad (5-5)$$

$$Z = 1.30 [1 + 0.010 (O.D. - 4)] \text{ (for SAW)} \quad (5-6)$$

where OD is the outer diameter in inches. Substituting OD = 14.00 inches, the Z factor was calculated to be 1.2995 for SMAW and 1.43 for SAW. The applied loads were increased by the Z factors and the plots of limit load versus crack length were generated as shown in figure 5-6 to 5-21. Tables 5-3 and 5-4 show the summary of critical flaw sizes for Sequoyah Units 1 & 2.

5.4 References

- 5-1 Kanninen, M. F. et al., "Mechanical Fracture Predictions for Sensitized Stainless Steel Piping with Circumferential Cracks" EPRI NP-192, September 1976.
- 5-2 [Fauske, H. K., "Critical Two-Phase, Steam Water Flows," Proceedings of the Heat Transfer and Fluid Mechanics Institute, Stanford, California, Stanford University Press, 1961.]^{a,c,e}
- 5-3 Tada, H., "The Effects of Shell Corrections on Stress Intensity Factors and the Crack Opening Area of Circumferential and a Longitudinal Through-Crack in a Pipe," Section II-1, NUREG/CR-3464, September 1983.
- 5-4 NRC letter from M. A. Miller to Georgia Power Company, J. P. O'Reilly, dated September 9, 1987.
- 5-5 ASME Code Section XI, Winter 1985 Addendum, Article IWB-3640.
- 5-6 Standard Review Plan; Public Comment Solicited; 3.6.3 Leak-Before-Break Evaluation Procedures; Federal Register/Vol. 52, No. 167/Friday, August 28, 1987/Notices, pp. 32626-32633.

TABLE 5-1

Leak Rate Crack Length for Sequoyah Unit 1

<u>Node Point</u>	<u>Load Case</u>	<u>Temperature</u> (°F)	<u>Crack Length (in.)</u> (for 10 gpm leakage)
1020	[a, c, e
1080	[a, c, e

TABLE 5-2

Leak Rate Crack Length for Sequoyah Unit 2

<u>Node Point</u>	<u>Load Case</u>	<u>Temperature</u> (°F)	<u>Crack Length (in.)</u> (for 10 gpm leakage)	
1020	[]	a, c, e
1080	[]	a, c, e

TABLE 5-3

Summary of Critical Flaw Size for Sequoyah Unit 1

<u>Node Point</u>	<u>Load Case</u>	<u>Temperature</u> (°F)	<u>Critical</u> <u>Flaw Size (in)</u>
1020	[a, c, e
1080	[a, c, e

TABLE 5-4

Summary of Critical Flaw Size for Sequoyah Unit 2

<u>Node Point</u>	<u>Load Case</u>	<u>Temperature</u> (°F)	<u>Critical</u> <u>Flaw Size (in)</u>	
1020	[]	a, c, e
1080	[]	a, c, e



Figure 5-1 Fully Plastic Stress Distribution

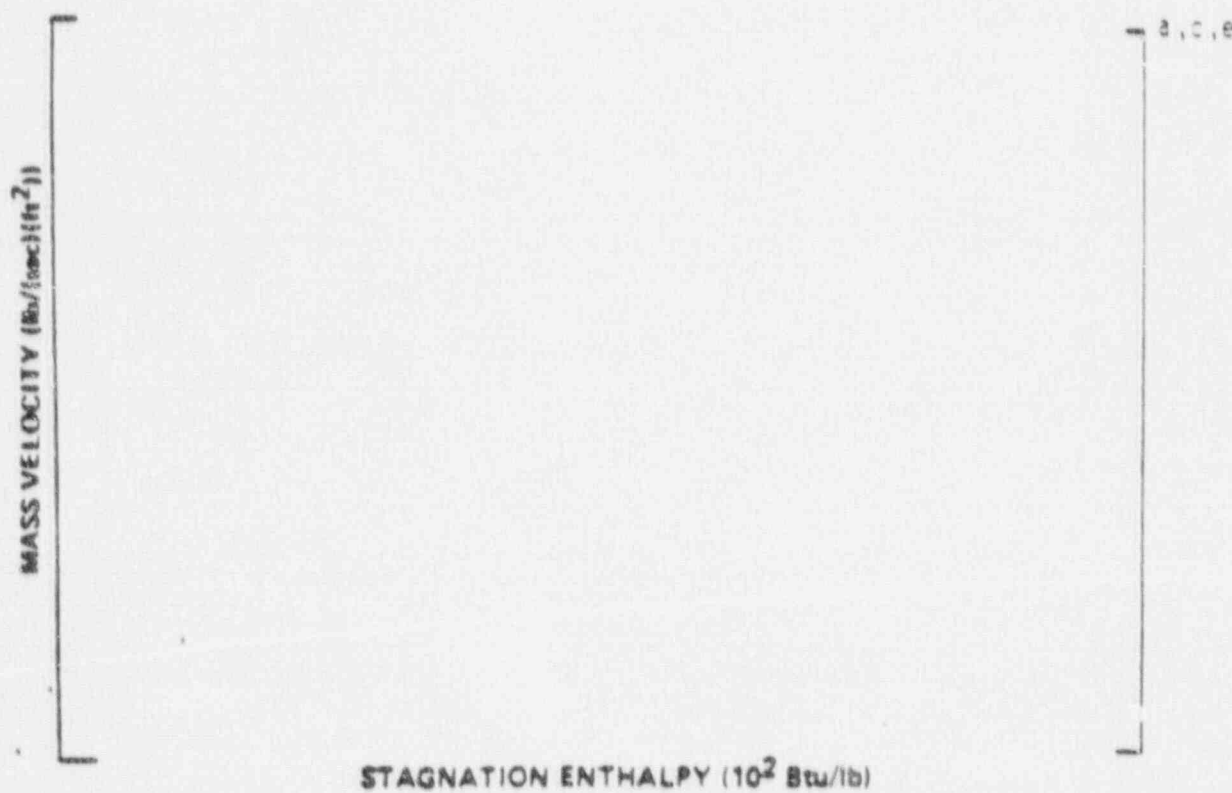


Figure 5-2 Analytical Predictions of Critical Flow Rates of
Steam-Water Mixtures

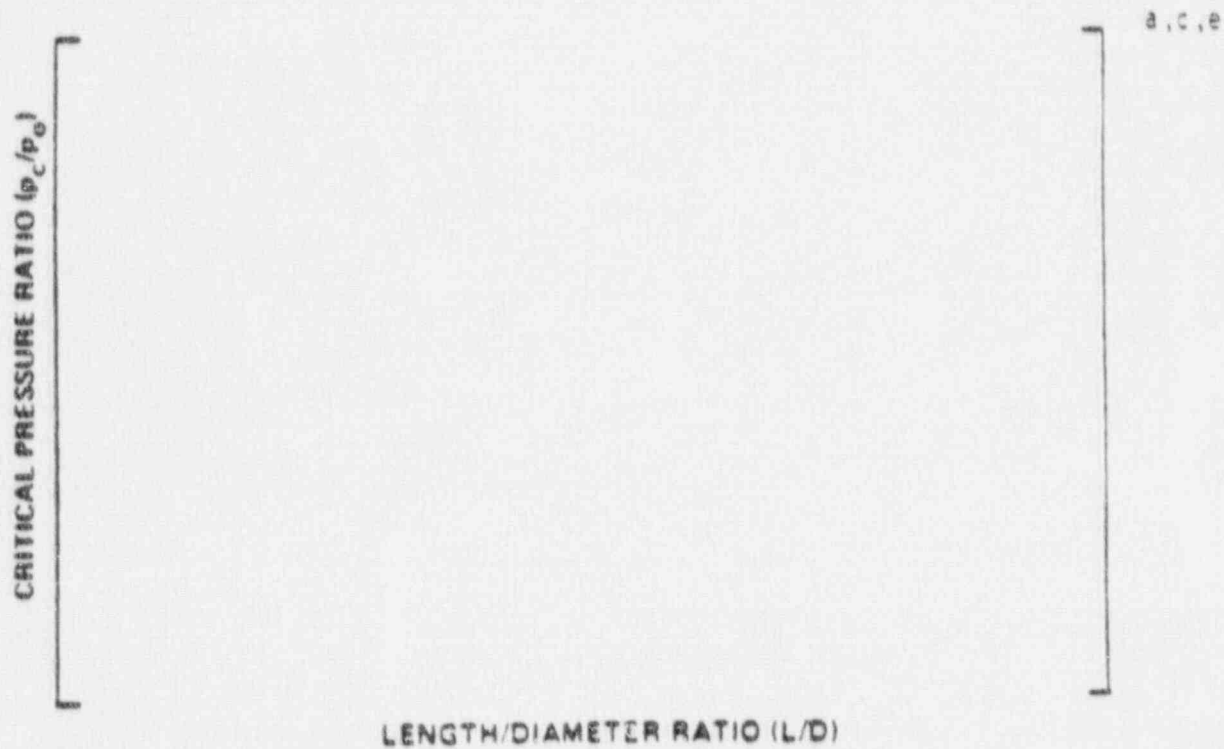


Figure 5-3 [] a, c, e Pressure Ratio as a Function of L/D

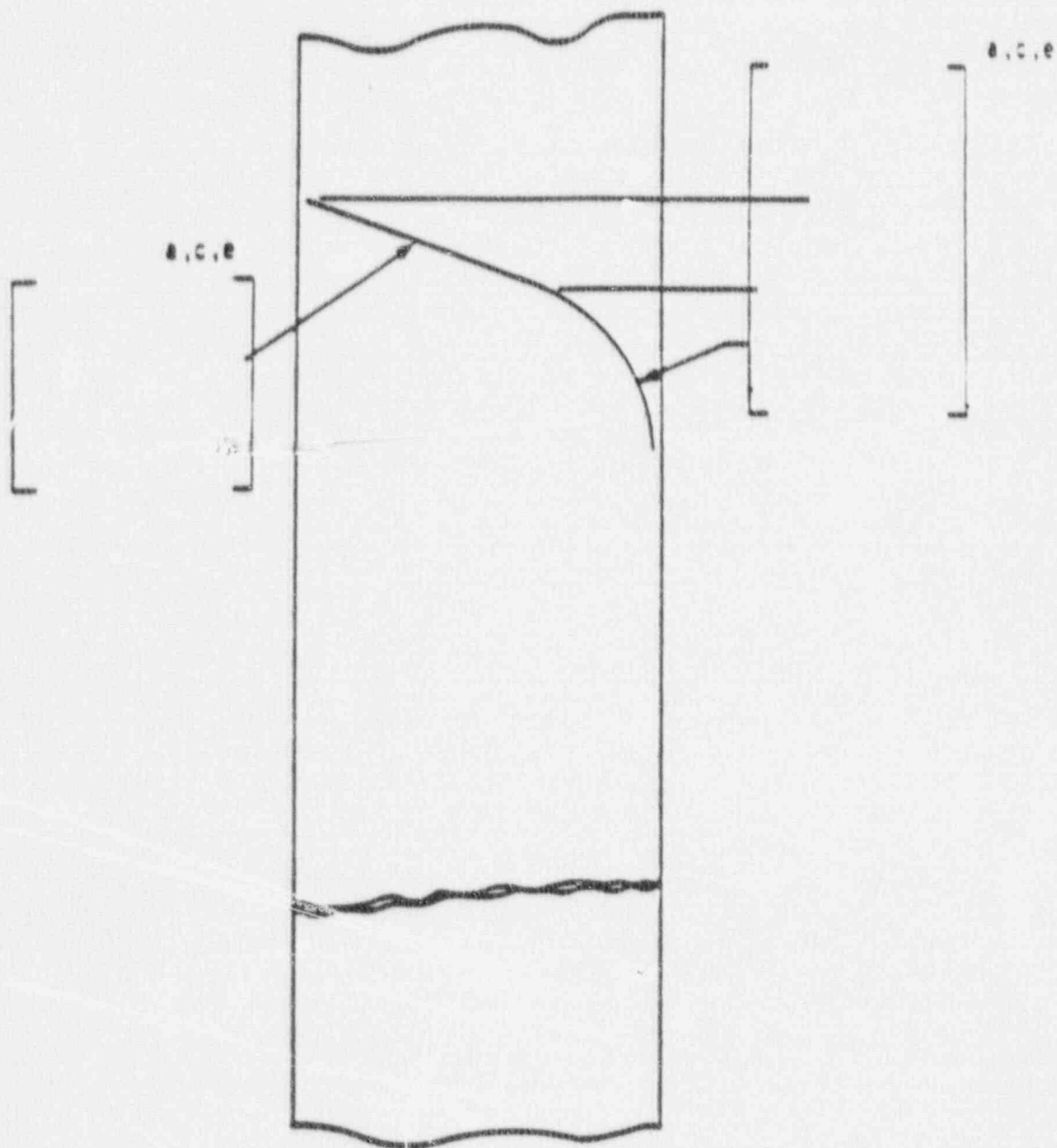


Figure 5-4. Idealized Pressure Drop Profile Through a Postulated Crack

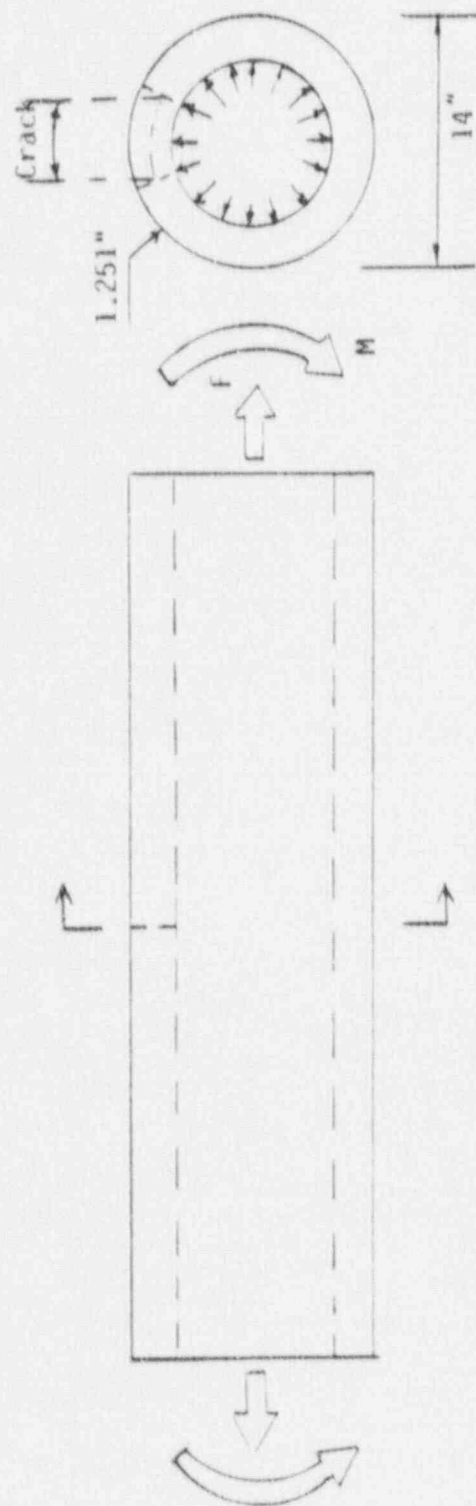


Figure 5-5. Loads Acting on the Model at the Governing Location

1,0,0

TVA NODE 1020 (SMAW) LOAD CASE D

PIPE OD=14.00 T=1.250 SIGY=24.6 SIGU=79.8 Fa=258.
M=.212E+04

Figure 5-6. Critical Flaw Size Prediction for Sequoyah Unit 1
Node 1020 Case D

a,c,e

TVA NODE 1020 (SMAW) LOAD CASE E

PIPE OD=14.00 T=1.250 SIGY=24.6

SIGU=79.8

Fa=258.

M=.214E+04

Figure 5-7. Critical Flaw Size Prediction for Sequoyah Unit 1
Node 1020 Case E

1, C, 2

TVA NODE 1020 (SMAW) LOAD CASE F

PIPE OD=14.00 T=1.250 SIGY=34.2

SIGU=83.3

Fa=56.1

M=.300E+04

Figure 5-8 Critical Flaw Size Prediction for Sequoyah Unit 1
Node 1020 Case F

a,c,e

TVA NODE 1020 (SMAW) LOAD CASE G

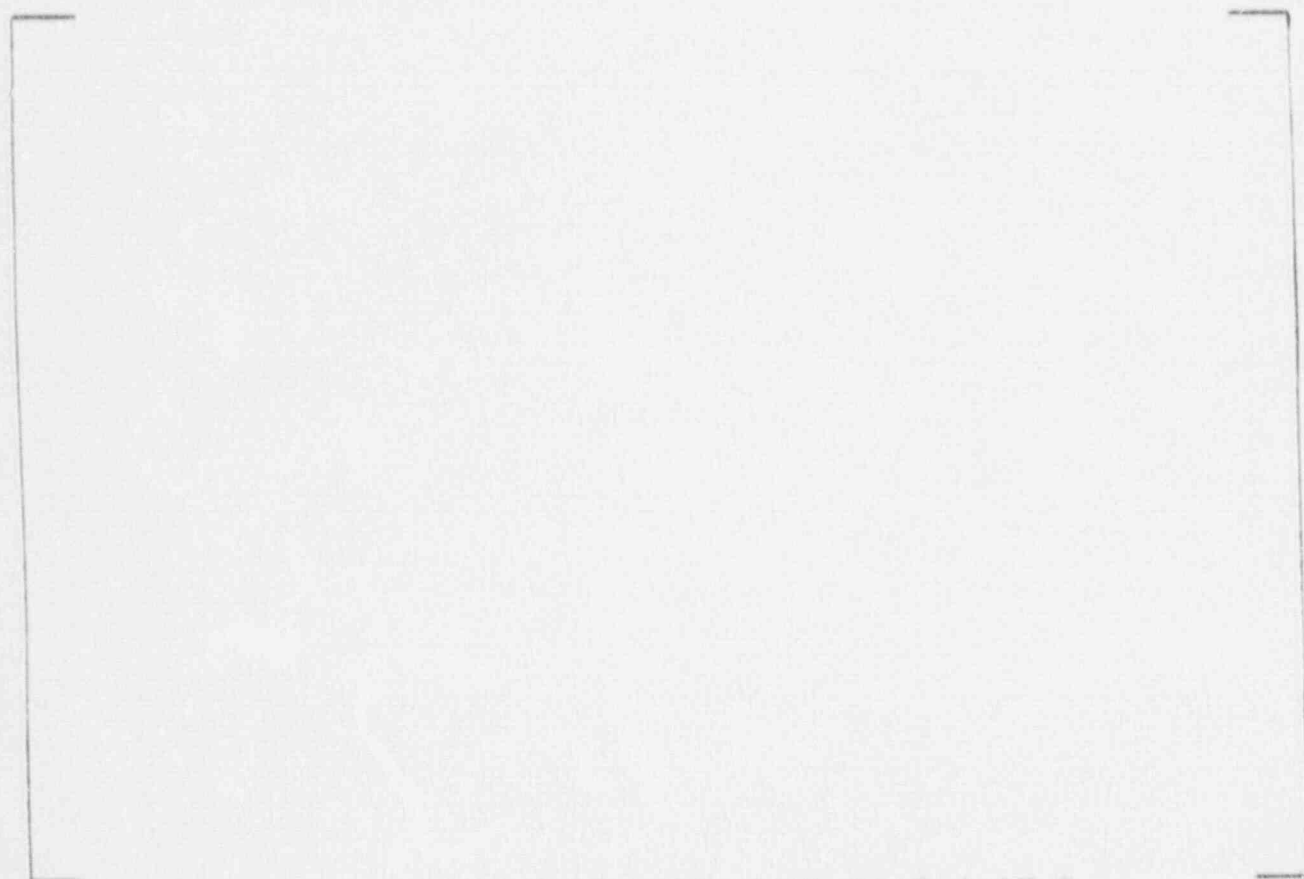
PIPE OD=14.00 T=1.250 SIGY=37.9

SIGU=83.4

Fa=61.8

M=.430E+04

Figure 5-9 Critical Flaw Size Prediction for Sequoyah Unit 1
Node 1020 Case G



TVA NODE 1080 (SAW) LOAD CASE D

PIPE OD=14.00 T=1.250 SIGY=24.6

SIGU=79.8

Fa=254.

M=.169E+04

Figure 5-10 Critical Flaw Size Prediction for Sequoyah Unit 1
Node 1080 Case D

d, c, e

TVA NODE 1680 (SAW) LOAD CASE E

PIPE OD=14.00 T=1.250 SIGY=24.6

SIGU=79.8

Fa=253.

M=.163E+04

Figure 5-11 Critical Flaw Size Prediction for Sequoyah Unit 1
Node 1080 Case E

a.c.e

TVA NODE 1080 (SAW) LOAD CASE F

PIPE OD=14.00 T=1.250 SIGY=30.2 SIGU=81.1 Fa=58.4
M=.227E+04

Figure 5-12 Critical Flaw Size Prediction for Sequoyah Unit 1
Node 1080 Case F

a,c,e

TVA NODE 1080 (SAW) LOAD CASE G

PIPE OD=14.00 T=1.250 SIGY=31.0

SIGU=81.6

Fa=63.3

M=.357E+04

Figure 5-13 Critical Flaw Size Prediction for Sequoyah Unit 1
Node 1080 Case G

a,c,e

TEN NODE 1020 (SMAW) LOAD CASE D

PIPE OD=14.00 T=1.250 SIGY=25.1

SIGU=79.5

Fa=258.

M=.212E+04

Figure 5-14. Critical Flaw Size Prediction for Sequoyah Unit 2
Node 1020 Case D

3.0.2

TEN NODE 1020 (SMAW) LOAD CASE E

PIPE OD=14.00 T=1.250 SIGY=25.1

SIGU=79.5

Fa=258.

M=.214E+04

Figure 5-15. Critical Flaw Size Prediction for Sequoyah Unit 2
Node 1020 Case E

a,c,e

TEN NODE 1020 (SMAW) LOAD CASE F

PIPE OD=14.00 T=1.250 SIGY=34.8

SIGU=82.9

f_a=56.1

M=.300E+04

Figure 5-16 Critical Flaw Size Prediction for Sequoyah Unit 2
Node 1020 Case F

TEN NODE 1020 (SMAW) LOAD CASE G

PIPE OD=14.00 T=1.250 SIGY=38.7

SIGU=83.0

Fa=61.8

M=.430E+04

Figure 5-17 Critical Flaw Size Prediction for Sequoyah Unit 2
Node 1020 Case G

TEN NODE 1080 (SAW) LOAD CASE D

PIPE OD=14.00 T=1.250 SIGY=25.1

SIGU=79.5

Fa=254.

M=.169E+04

Figure 5-18 Critical Flaw Size Prediction for Sequoyah Unit 2
Node 1080 Case D

3.0.2

TEN NODE 1080 (SAW) LOAD CASE E

PIPE OD=14.00 T=1.250 SIGY=25.1

SIGU=79.5

Fa=253.

M=.163E+04

Figure 5-19 Critical Flaw Size Prediction for Sequoyah Unit 2
Node 1080 Case E

B.C.2

TEN NODE 1080 (SAW) LOAD CASE F

PIPE OD=14.00 T=1.250 SIGY=30.8

SIGU=80.7

Fa=58.4

M=.227E+04

Figure 5-20 Critical Flaw Size Prediction for Sequoyah Unit 2
Node 1080 Case F

TEN NODE 1080 (SAW) LOAD CASE G

PIPE OD=14.00 T=1.250 SIGY=31.6

SIGU=81.2

Fa=63.3

M=.357E+04

Figure 5-21 Critical Flaw Size Prediction for Sequoyah Unit 2
Node 1080 Case G

SECTION 6.0 ASSESSMENT OF FATIGUE CRACK GROWTH

6.1 Introduction

To determine the sensitivity of the pressurizer surge line to the presence of small cracks when subjected to the transients discussed in WCAP-12777, fatigue crack growth analyses were performed. This section summarizes the analyses and results.

Figure 6-1 presents a general flow diagram of the overall process. The methodology consists of seven basic steps as shown in figure 6-2. Steps 1 through 4 are discussed in WCAP-12777. Steps 5 through 7 are specific to fatigue crack growth and are discussed in this section.

There is presently no fatigue crack growth rate curve in the ASME Code for austenitic stainless steels in a water environment. However, a great deal of work has been done recently which supports the development of such a curve. An extensive study was performed by the Materials Property Council Working Group on Reference Fatigue Crack Growth concerning the crack growth behavior of these steels in air environments, published in reference 6-1. A reference curve for stainless steels in air environments, based on this work, is in the 1989 Edition of Section XI of the ASME Code. This curve is shown in figure 6-3.

A compilation of data for austenitic stainless steels in a PWR water environment was made by Bamford (reference 6-2), and it was found that the effect of the environment on the crack growth rate was very small. For this reason it was estimated that the environmental factor should be set at 1.0 in the crack growth rate equation from reference 6-1. Based on these works (references 6-1 and 6-2) the fatigue crack growth law used in the analyses is as shown in figure 6-4.

6.2 Initial Flaw Size

Various initial surface flaws were assumed to exist. The flaws were assumed to be semi-elliptical with a six-to-one aspect ratio. The largest initial flaw assumed to exist was one with a depth equal to 10% of the nominal wall thickness, the maximum flaw size that could be found acceptable by Section XI of the ASME Code.

6.3 Results of FCG Analysis

Fatigue crack growth analyses were performed at the reactor coolant loop nozzle junction at location 1 (which corresponds to the highest usage factor in the surge line) and at location 2 as shown in Figure 6-5. Location 2 corresponds to the location of highest ASME Section III equation 12 stress.

Results of the fatigue crack growth analysis are presented in table 6-1 for an initial flaw of 10% nominal wall thickness.

Conservatisms existing in the fatigue crack growth analysis are listed below.

1. Plant operational transient data has shown that the conventional design transients contain significant conservatisms
- [2.
- 3.
- a,c,e
4. Fatigue crack growth calculations are based conservatively on elastic stresses
5. FCG neglects fatigue life prior to initiation

6.4 References

- 6-1. James, L. A. and Jones, D. P., "Fatigue Crack Growth Correlations for Austenitic Stainless Steel in Air," in Predictive Capabilities in Environmentally Assisted Cracking, ASME publication PVP-99, December 1985.
- 6-2. Bamford, W. H., "Fatigue Crack Growth of Stainless Steel Reactor Coolant Piping in a Pressurized Water Reactor Environment," ASME Trans. Journal of Pressure Vessel Technology, Feb. 1979.

TABLE 6-1

FATIGUE CRACK GROWTH RESULTS FOR 10% of WALL INITIAL FLAW SIZE

Location	Position	Initial Size (in)	Initial (% Wall)	Final (40 yr) Size (in)	Final Flaw (% Wal)
----------	----------	----------------------	---------------------	----------------------------	-----------------------

a,c,e

DETERMINATION OF THE EFFECTS OF THERMAL STRATIFICATION

a,c,e

Figure 6-1 Determination of the Effects of Thermal Stratification on Fatigue Crack Growth

a.c.e

Figure 6-2 Fatigue Crack Growth Methodology

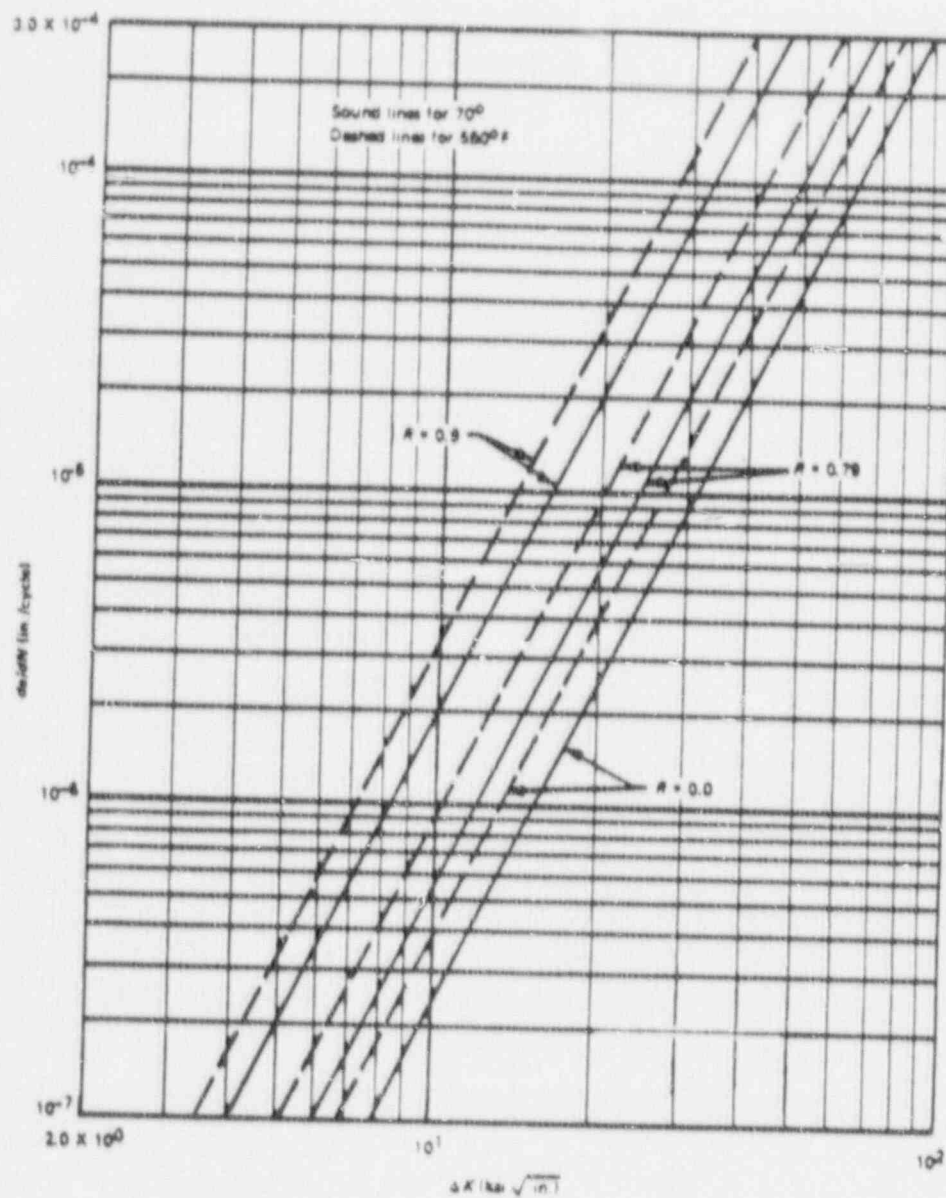


Figure 6-3 Fatigue Crack Growth Rate Curve for Austenitic Stainless Steel

$$\frac{da}{dn} = C F S E \Delta K^{3.30}$$

where

$\frac{da}{dn}$ = Crack Growth Rate in inches/cycle

C = 2.42×10^{-20}

F = Frequency factor (F = 1.0 for temperature below 800°F)

S = R ratio correction (S = 1.0 for R = 0; S = $1 + 1.8R$ for $0 < R < .8$; and S = $-43.35 + 57.97R$ for $R > 0.8$)

E = Environmental Factor (E = 1.0 for PWR)

ΔK = Range of stress intensity factor, in psi $\sqrt{\text{in}}$

R = The ratio of the minimum K_I (K_{Imin}) to the maximum K_I (K_{Imax}).

Figure 6-4. Fatigue Crack Growth Equation for Austenitic Stainless Steel

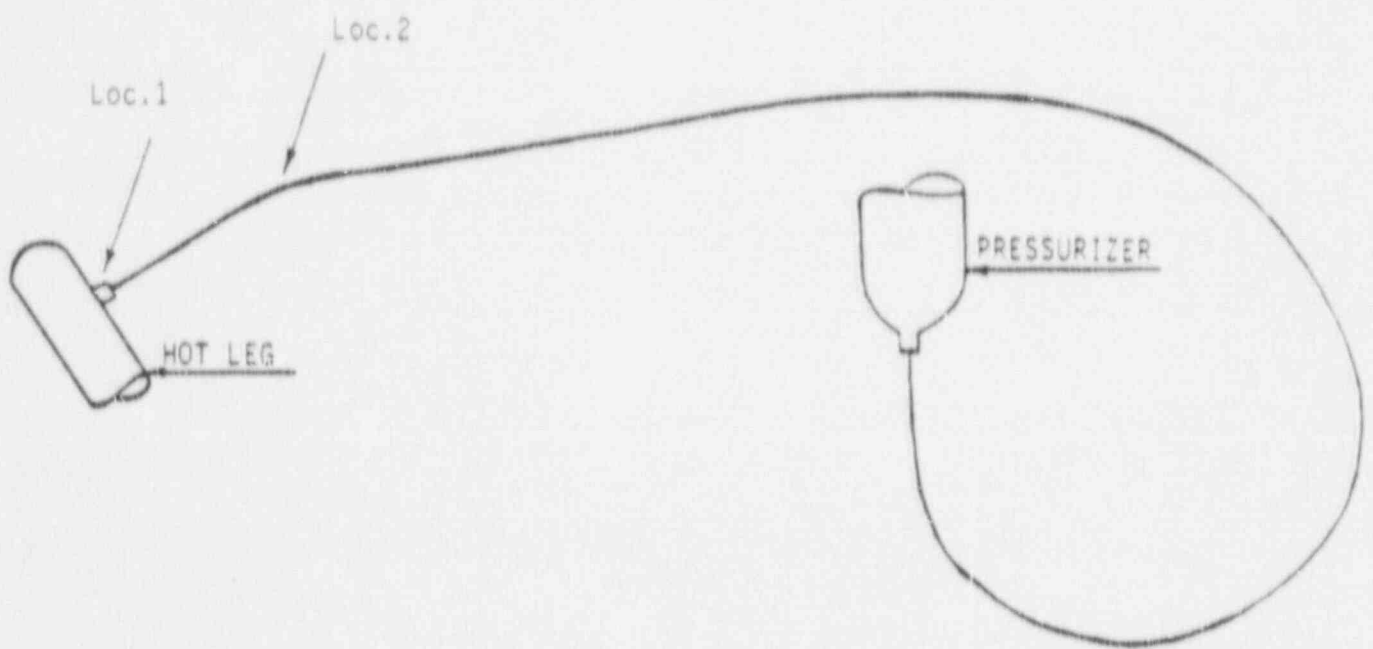


Figure 6-5. Fatigue Crack Growth Critical Locations

SECTION 7.0 ASSESSMENT OF MARGINS

In the preceding sections, the leak rate calculations, fracture mechanics analysis and fatigue crack growth assessment were performed. Margins at the critical locations are summarized below:

In Section 5.3 using the IWB-3640 approach (i.e. "Z" factor approach), the "critical" flaw sizes at the governing locations are calculated. In Section 5.2 the crack lengths yielding a leak rate of 10 gpm (10 times the leak detection capability of 1.0 gpm) for the critical locations are calculated. The leakage size flaws, the instability flaws, and margins are given in Tables 7-1 and 7-2. The margins are the ratio of instability flaw to leakage flaw. The margins for analysis combination cases A/D, []^{a,c,e} well exceed the factor of 2. The margin for the extremely low probability event defined by []^{a,c,e} has also exceeded the factor of 2. As stated in Section 4.3, the probability of simultaneous occurrence of SSE and maximum stratification due to shutdown because of leakage is estimated to be very low.

In this evaluation, the leak-before-break methodology is applied conservatively. The conservatisms used in the evaluation are summarized in Table 7-3.

TABLE 7-1

Leakage Flaw Sizes, Critical Flaw Sizes and Margins
for Sequoyah Unit 1

<u>Node</u>	<u>Load Case</u>	<u>Critical Flaw Size (in)</u>	<u>Leakage Flaw Size (in)</u>	<u>Margin</u>
1020	A/D	14.60	3.80	3.84
	A/F	[] a,c,e
	B/E			
	B/F			
	C/G ^a			
	B/G ^a			
1080	A/D	15.08	5.55	2.72
	A/F	[] a,c,e
	B/E			
	B/F			
	C/G ^a			
	B/G ^a			

^a These are judged to be low probability events

TABLE 7-2

Leakage Flaw Sizes, Critical Flaw Sizes and Margins
for Sequoyah Unit 2

<u>Node</u>	<u>Load Case</u>	<u>Critical Flaw Size (in)</u>	<u>Leakage Flaw Size (in)</u>	<u>Margin</u>
1020	A/D	14.61	3.70	3.94
				a, c, e
1080	A/D	15.09	5.50	2.74
				a, c, e

^a These are judged to be low probability events

TABLE 7-3

LBB Conservatisms

- o Factor of 10 on Leak Rate
- o Factor of 2 on Leakage Flow for all cases
- o Algebraic Sum of Loads for Leakage
- o Absolute Sum of Loads for Stability
- o Average Material Properties for Leakage
- o Minimum Material Properties for Stability

SECTION 8.0 CONCLUSIONS

This report justifies the elimination of pressurizer surge line pipe breaks as the structural design basis for Sequoyah Units 1 and 2 as follows:

- a. Stress corrosion cracking is precluded by use of fracture resistant materials in the piping system and controls on reactor coolant chemistry, temperature, pressure, and flow during normal operation.
- b. Water hammer should not occur in the RCS piping (primary loop and the attached class 1 auxiliary lines) because of system design, testing, and operational considerations.
- c. The effects of low and high cycle fatigue on the integrity of the surge line were evaluated and shown acceptable. The effects of thermal stratification were evaluated and shown acceptable.
- d. Ample margin exists between the leak rate of small stable flaws and the criterion of Reg. Guide 1.45.
- e. Ample margin exists between the small stable flaw sizes of item d and the critical flaw size.
- f. With respect to stability of the reference flaw, ample margin exists between the maximum postulated loads and the plant specific maximum faulted loads.

The postulated reference flaw will be stable because of the ample margins in d, e and f and will leak at a detectable rate which will assure a safe plant shutdown.

Based on the above, it is concluded that pressurizer surge line breaks should not be considered in the structural design basis of Sequoyah Units 1 & 2.

APPENDIX A

LIMIT MOMENT

APPENDIX A
LIMIT MOMENT

I

a,c,e

a.c.e

Figure A-1. Pipe With A Through Wall Crack In Bending